25th ABCM International Congress of Mechanical Engineering
October 20-25, 2019, Uberlândia, MG, Brazil

COB-2019-0061
DECODING IMAGINARY ELBOW MOVEMENT WITH KALMAN FILTER USING NON-INVASIVE *EEG*

E.Y. Veslin
M.S. Dutra
L. Bevilacqua
R.S. Figueiredo
Universidade Federal do Rio de Janeiro, Av. Horácio Macedo 2030, Centro de Tecnologia, Bloco G, sala 101, Cidade Universitária, CEP 21941-914, Rio de Janeiro, RJ, Brasil
elkinveslin@ufrj.br, max@mecanica.coppe.ufrj.br , bevilacqua@coc.ufrj.br, rafaelsfigueiredo@ufrj.br

L.S.C. Raptopoulos
W.S. Andrade
NUPEM/CEFET-RJ – Núcleo de Pesquisa em Mecatrônica do Centro Federal de Educação Tecnológica Celso Suckow da Fonseca, Estr. de Adrianópolis 1317, CEP 26041-271, Nova Iguaçu, RJ, Brasil
luciano.raptopoulos@cefet-rj.br

J.G.M. Soares
Universidade Federal do Rio de Janeiro, Av. Carlos Chagas Filho, 373, Centro de Ciências da Saúde, Bloco G, sala G1-019, Cidade Universitária, CEP 21941-902, Rio de Janeiro, RJ, Brasil
jmsoares@biof.ufrj.br

Abstract. *In this article, the properties of the Kalman Filter to decode imaginary elbow movement from non-invasive EEG are analyzed. Based on a set of executed movements, an expected interval of movement during imagination is estimated, together, with a set of signal's configuration parameters and trough cross-validation the decoded capabilities are analyzed in order to generalize the model that reduces the estimation error around all the volunteers. We found that selecting the parameters correctly to configure the signals and selecting a homogeneous data set is possible to improve the filter estimation capabilities for imaginary movement.*

Keywords: *EEG Signals, Kalman Filter, Brain-machine interfaces, Decoding, Imaginary Movement*

1. INTRODUCTION

The interpretation and use of brain patterns related to cognitive tasks is the basis of the Brain-Computer Interfaces (*BCI*) and Brain-Machine Interfaces (*BMI*). Neural patterns related to motor control, imagination and movement intention have been identified, and, integrated through *BCI* systems to control mechanisms destined to movement assistance in disabled persons with a partial or total restriction on the movement of their limbs. Examples of such devices are: exoskeletons Soekadar *et al.* (2015), Lalitharatne *et al.* (2012), wheelchairs Zhang *et al.* (2016) or robotic manipulators Roy *et al.* (2016).

The alpha band activity (8-15 Hz) is one of the most prominent signals of the motor cortex related to body movement and imagination used in *BMI* systems Frolov *et al.* (2013). It had commonly used in classification task Besserve *et al.* (2007) to identify motion execution, and most recently, motion decoding Korik *et al.* (2018). Previous works, had been reported that alpha-band energy decreases during voluntary movement Cassim *et al.* (2000),Robinson *et al.* (2013), imaginary movement (IM) Pfurtscheller *et al.* (2006) and even, visualized movement Lana *et al.* (2015), in relation to an alteration in the frequency oscillation Pfurtscheller and da Silva (1999), this related event is called as desynchronization (*ERD*). It has been reported that during the execution of real and imaginary movements Salvaris and Sepulveda (2010), Ramos-Murguialday and Birbaumer (2015) similar brain patterns are presented, suggesting that the same cortical areas are activated in the presentation of the event, in both cases occurring a desynchronization during limb movement followed by a synchronization (*ERS*) when it ends Jeon *et al.* (2011).

On the other hand, the kinematics decoding consists of the reconstruction of motion from biological signals. Previous studies had demonstrated the possibility to decode kinematics from *EEG* signals, and consequently, achieve a continuous motion reconstruction that could be applied into *BMI* systems. The first attempts to create a model to reconstruct

continuous motion are found in Georgopoulos *et al.* (1986), where was demonstrated that *M1* cells firing rates are related to the movement direction in center-out hand movements. These firing rates were more intense with movements executed in a preferred direction and gradually decrease as it went far. Mathematical models that establish a relationship between the tuning of the cell and the direction were developed in Georgopoulos *et al.* (1986); subsequently, a model that includes the hand velocity was introduced by Moran and Schwartz (1999).

Based in this neural behavior, diverse decoding techniques had been applied to reconstruct motion from various kinematics task using invasive or non-invasive techniques. One of the most implemented decoding algorithm is the multidimensional linear regression, also knows as Wiener filter. This filter was implemented in Lalitharatne *et al.* (2012) and Ubeda *et al.* (2015). This technique allows to decode a movement in an instant of time t using a set of delayed data. Other techniques used for decoding are the neural networks Tang *et al.* (2014), Tayeb *et al.* (2019) and Shakibaee *et al.* (2019); deep learning Rao (2019); and the Kalman filter Wu *et al.* (2002), Ubeda *et al.* (2015) and Robinson *et al.* (2015). Through this methods had been possible to estimate from *EEG* diverse kinematic task as: hand speed Lv *et al.* (2010), elbow velocity Lalitharatne *et al.* (2013), movement imagination Korik *et al.* (2018), Tayeb *et al.* (2019), Li *et al.* (2019), finger movement Alazrai *et al.* (2019), elbow motion Veslin *et al.* (2019), and hand position Ofner and Müller-Putz (2012), Ubeda *et al.* (2015).

Decoding from imaginary limb motion is a new research area. Current *BCI* systems use sensorimotor rhythms to discriminate (classify) between two or more different imaginary motions Müller-Putz *et al.* (2016), however, advances in imaginary decoding could be found in Ofner and Müller-Putz (2015), where imagined rhythmic arm movement in the vertical and horizontal plane was estimated using linear filters. In Korik *et al.* (2014), were found a correlation between *EEG* and 3D hand movements in both imaginary and real motion. Sub-bands in the 0.5-4 Hz and 28-36 Hz showed the highest level of correlation with movement trajectory, making them plausible to be used in decoding of 3D hand motion trajectories using linear filters Korik *et al.* (2018).

Difficulties in decoding from imaginary motion are related to associate the cognitive activity to a trajectory or action. Related studies aim to associate the signals with a non-arbitrary motion that are intended to be made. In order to do that, have been considered the decoding from task observation Hochberg *et al.* (2012), Kim *et al.* (2014), and voluntary movement imagination Kim *et al.* (2014), Ofner and Müller-Putz (2015), Korik *et al.* (2018). In the related cases, the decoded motion is associated with the brain patterns response using as reference an expected path. According to Müller-Putz *et al.* (2016), the movements decoded by the *BMI-BCI* need to be closely related to the user's intention, thereby, assistive devices could achieve a more natural control if the decoded signals are originating from sensorimotor activity related to voluntary or imaginary movement.

1.1 Kalman Filter

In Wu *et al.* (2002), a method for decoding 2-D hand movement from primates neural activity through a generative model in a Bayesian approach was introduced. This approach allowed to decode multiple kinematic variables from invasive *EEG*, enhancing the estimation performance in comparison with works that decoded kinematics from linear filters.

From there, Kalman Filter was successfully applied to decode hand movement trajectories using Electrocorticography (*ECoG*) Pistohl *et al.* (2008), hand velocity Lv *et al.* (2010), position and velocity of a cursor in a screen Homer *et al.* (2013), control of virtual robotic arms Moorman *et al.* (2017), and control of a robotic arm by patients with tetraplegia Hochberg *et al.* (2012). However, Kalman decoding based in non-invasive readings are not enough explored, but recent findings in 2-D hand movement Robinson and Vinod (2016), Robinson *et al.* (2015), and human gait Luu *et al.* (2016) could be found, suggesting that high dimensional cell recordings made from external reading devices maintain the properties and therefore, it is possible to decode motion despite the higher *SNR*. On the other hand, Kalman Filter had not been considered to decode imaginary motion, is it applied to decode visualized movement with a limited success Hochberg *et al.* (2012).

In Veslin *et al.* (2019) was found that the incidence of the decoding precision when a Liner Kalman Filter is used to decode is depending on the movement data set, therefore, the use of trials with high motion variance in velocity and acceleration train filters with lower decoding capability. To increase the decoding precision was found that the training data set must be composed of movement recordings whit lower variance, disposing of them trials that were made with high speed. However, this effect only could be observed in commanded motion when the system forces the volunteer to perform a predefined path. Therefore, in cases as imaginary motion decoding, the effect of state selection could be applied, as the relative *EEG* patterns related to imagery are used to estimate a trajectory which is build of a reference motion data sets.

In this work, we propose to apply the Kalman Filter to decode imaginary right elbow flexion/extension movement using non-invasive *EEG* recordings. The filter model is tested through cross-validation techniques determining a set of signal configuration parameters used to optimize the decoding result. The results are analyzed using the *Mean Squared Error* (*MSE*). According to the selected parameters, the proposed filter is studied concerning a set of reference trajectories of higher and lower variance. The decoding response for the data set is analyzed through graphics. This work expects to

analyze the influence of the data set into decoding response and give highlights to future projects.

2. Materials and Methods

2.1 Experiment Paradigm

This study was conducted following the protocol approved by the Ethics Committee of *Federal University of Rio de Janeiro* (Approbation number: 851.521). Seven healthy right-handed volunteers (6 females and one male), without previous training in similar procedures, were studied. In the test, the volunteer is seated on a chair, with their arms in a rest position in a conditioned room (Fig. 1 right). A screen was used to present the instructions, which were randomly generated to prevent any action anticipation. The instructions consisted of two tasks: real and imaginary arm movement, consolidating 60 trials of 10 seconds of duration.

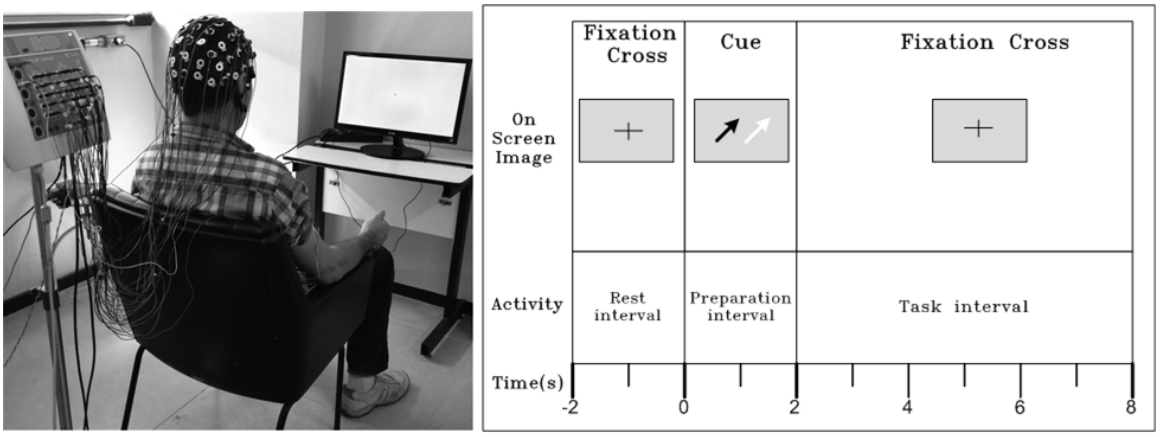

Figure 1. Volunteer disposition in front of the command screen (a). Description of the trial, referencing the on-screen image during the interval and the activity developed by the volunteer (b). The cue arrow color commands the task: black for real and white for imaginary.

The trial sequence is described in Fig. 1 left, it begins with the presentation of a fixation cross at the center of the screen during 2 seconds indicating to the volunteer to wait for the instruction (rest interval). Then, the cross is replaced during 2 seconds by an instructive arrow indicating the volunteer which task must be performed (preparation interval). Then, the arrow is replaced by the fixation cross, reporting to the subject to execute the instruction within a 6 seconds interval (task interval). A real movement consisted of the right elbow flexion/extension on the range of 90°to 150°approximately. The action was uniquely executed when a black arrow appeared on the screen; a white arrow indicates to the volunteer to imagine the task execution. The task interval duration was configured so that it was as long as the brain activity and the elbow returned to a rest state Pfurtscheller and da Silva (1999). The volunteer was instructed to perform the imaginary movement in the first person, trying to replicate the action performed in real trials.

2.2 *EEG* recording and signal processing

The *EEG* was recorded continuously from scalp electrodes using the *Neuron-Spectrum* system and software (Neurosoft Ltd, Ivanovo, Russia). A total of 32 passive *Ag-AgCl* electrodes were distributed around the scalp using a *MCScap* (Medical Computer Systems Ltd, Moscow, Russia) with removable electrodes according to a 10-10 modified system (Fig. 2). During the experiment, their impedance was kept below 10K Ω. The system was referenced to two interlinked ear reference $(A_1 - A_2)$. An additional *EMG* electrodes monitored the muscular activity in the biceps. A *MPU6050* accelerometer located in the forearm was used to read the angular position when real movements were executed. The velocity and acceleration were obtained through signal processing.

The signals were amplified, digitized with a sampling rate of 1000 Hz and band-pass filtered in the 0.5-100 Hz frequency band. *EEG* data were preprocessed using the *EEGLAB* Matlab toolbox. Artifacts, as eye blinking and head movements presented as components with homogeneous contributions, were removed using the *ICA* algorithm of the *EEGLAB* toolbox. The artifacts were removed using *runica* as decomposition method through the 10 seconds test in all the recorded trials. Segments with high signal interference or disturb were also removed. Finally, a fourth-order pass-band filter in the 1 to 55 Hz band was applied.

Data sets of *EEG* signals and sensor movement were prepared. Due to their relationship to motor control, *EEG* signals in the mu band were considered, thus, a fourth-order pass-band filter in the 8 to 13 Hz band was applied. As Kalman filter assumes that signals have Gaussian distribution, the filtered *EEG* signals were squared rooted transformed Wu *et al.* (2006). Motion signal was filtered into the 60 Hz frequency using a notch filter. To extract the velocity and acceleration, it

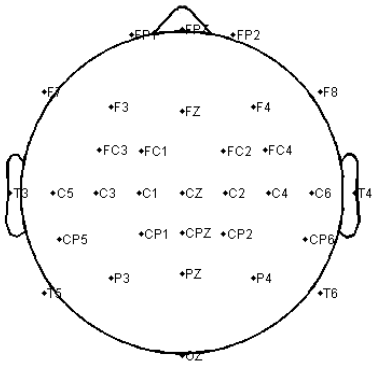

Figure 2. Location of the 32 channels around the scalp, the electrodes were distributed according to a 10-10 System with modifications. Source *EEGLAB*.

was derivative and divided by the period to obtain the real magnitudes. Finally, both sets were centralized by subtracting the mean value Wu *et al.* (2006). To get the movement time interval was implemented a muscle activation detector in the *EMG* signal using the algorithm described in Xu and Adler (2004).

3. The Kalman Filter

The decoding model has as purpose to estimate the state $\mathbf{x}_k$ in the time instant t_k. The states represent right elbow angular position, velocity and acceleration. As a measured signal, the notation $\mathbf{z} \in \Re^C$ is used, where *C* stands for the number of *EEG* electrodes used to decode the elbow kinematic.

According to Wu *et al.* (2002) the filter is determined assuming a linear relationship between the state $\mathbf{x}_k$ and the observations $\mathbf{z}_k$ in the instant of time t_k. The generative model is then stated in Eq. 1 as:

$$\mathbf{z}_k = \mathbf{H}_k \mathbf{x}_k + \mathbf{v}_k \tag{1}$$

Where $\mathbf{H}_k \in \Re^{C\times 3}$ is a matrix that linearly relates the neural activity captured from the *EEG* electrodes with the kinematics. A Gaussian noise $\mathbf{v}_k$ described as a normal distribution whit zero mean and covariance matrix $\mathbf{R}_k \in \Re^{C\times C}$, $\mathbf{v}_k \sim (0, \mathbf{R}_k)$.

The state $\mathbf{x}_k$ propagates in time according to the model described in Eq. 2 as:

$$\mathbf{x}_{k+1} = \mathbf{A}_k \mathbf{x}_k + \mathbf{w}_k \tag{2}$$

Where $\mathbf{A}_k \in \Re^{3\times 3}$ is a matrix that linearly relates the kinematics between times k and $k+1$. The noise term $\mathbf{w}_k$ is assumed to have a normal distribution with zero mean and covariance $\mathbf{Q}_k \in \Re^{3\times 3}$, $\mathbf{w}_k \sim (0, \mathbf{Q}_k)$.

3.1 Training Process

To train the matrices $\mathbf{A}_k, \mathbf{H}_k$, $\mathbf{R}_k$ and $\mathbf{Q}_k$ was assumed that the models in Eq. 1 and Eq. 2 are invariant along time. Considering that the signals $\mathbf{x}_k$ and $\mathbf{z}_k$ have a length $k = 1 \dots M$ and using least squares Wu *et al.* (2002), the solutions for matrix $\mathbf{A}$ and $\mathbf{H}$ are expressed in 3 as:

$$\begin{aligned} \mathbf{A} &= \mathbf{X}_2 \mathbf{X}_1^T (\mathbf{X}_1 \mathbf{X}_1^T)^{-1} \\ \mathbf{H} &= \mathbf{Z}\mathbf{X}^T (\mathbf{X}\mathbf{X}^T)^{-1} \end{aligned} \tag{3}$$

Using the learned values of $\mathbf{A}$ and $\mathbf{H}$ the noise covariance are then determined as is described in Eq. 4:

$$\begin{aligned} \mathbf{Q} &= \frac{(\mathbf{X}_2 - \mathbf{A}\mathbf{X}_1)(\mathbf{X}_2 - \mathbf{A}\mathbf{X}_1)^T}{(M-1)} \\ \mathbf{R} &= \frac{(\mathbf{Z} - \mathbf{H}\mathbf{X})(\mathbf{Z} - \mathbf{H}\mathbf{X})^T}{M} \end{aligned} \tag{4}$$

Where the matrix $\mathbf{X} \in \Re^{3\times M}$ correspond to the state values, matrix $\mathbf{X}_1 \in \Re^{3\times M-1}$ represents the state values from time interval $k = 1 \dots M-1$, the matrix $\mathbf{Z} \in \Re^{C\times M}$ is the *EEG* signals from the C channels, and the matrix $\mathbf{X}_2 \in \Re^{3,M-1}$ stands for the state values taken from the time interval $k = 2 \dots M$.

Matrices $\mathbf{A}, \mathbf{H}$, $\mathbf{R}$ and $\mathbf{Q}$ coefficients are dependents of the training data. This data could be configured according to a set of parameters, being them the number of channels C and the step time Δ_t. As different combinations could be made, 6-fold cross-validation was done to determine which combination performs the best decoding result. The selected parameters were the ones that minimized the decoding error represented as the Mean Squared Error (*MSE*) who is defined in Eq. 5 as:

$$MSE = \frac{1}{M}\sum_{k=1}^{M}(\mathbf{x}_k - \hat{\mathbf{x}}_k)^2 \tag{5}$$

Where $\hat{\mathbf{x}}_k$ represents the estimated state in t_k, being M the toal number of decoded points .

Due to being an imaginary process, no real motion could be extracted from this trial. Thus, we used motion data sets from the trials to determine a mean movement interval and trajectory for each volunteer, as is described in Fig. 3. Two principal data sets are processed: for real movement trials, the *EMG* and the accelerometer signals are extracted. They are used to determine the mean states and their respective time interval. Those signals will be used with the *EEG* signals originating from Imaginary trials to train the Kalman Filter. The resultant trained model is used to validate the decoding performance.

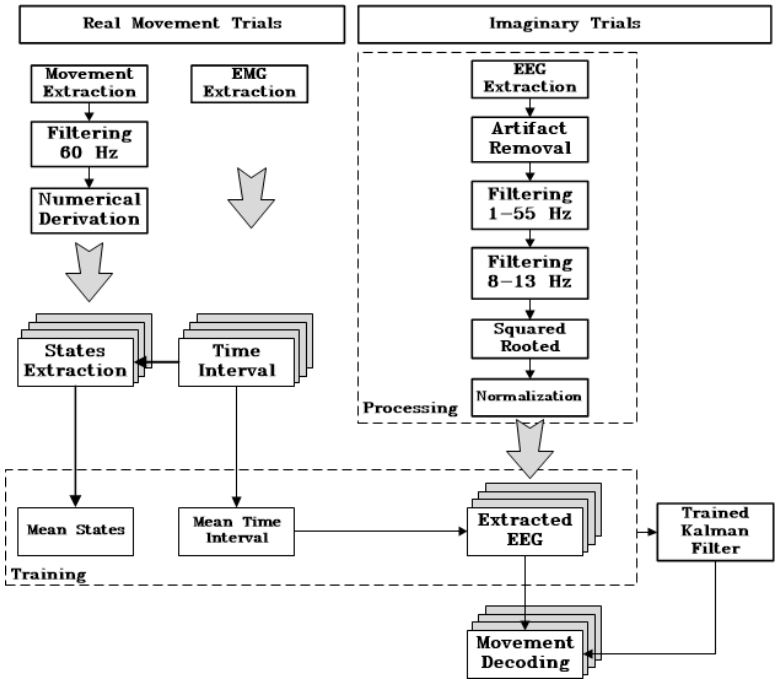

Figure 3. Procedure Data Flow. The diagram describes the steps to decode the imaginary movement in each volunteer.

In this work, two generative models were built, one that decodes flexion and another for the extension. Therefore, a learning method for each task was done, to do that, sections of *EEG* signals corresponding to the time interval where the task was executed were separated and used to train the models. This action is performed in each volunteer's data set.

4. Results

4.1 Cross-validation

Before initiating the cross-validation, the channels were rearranged in descendant form according to the coherence respect to C_3 channel. This reference was made as its location is closer to the cortex area where the right arm movement is controlled Noback *et al.* (2005). The channel organization was generalized for each volunteer, according to the trial's mean coherence value; this was made to reduce the processing time during the test. The cross-validation was performed dividing by the volunteer's data set in 6-folds of 10 trials each one.

In Fig. 4 the error curves obtained for ascending movements are presented, testing Δ_t (left) values from 1 to 200 ms, and sets of channels C from 3 to 34 (right). In the left figure, the error curve presents the mean *MSE* from the training set (bold line) and the validation set (dashed line), the horizontal lines present the inter volunteers variance from validation and training. A red square presents an augmentation of the zone. In the right figure is presented only the mean *MSE* for the validation set respect to each combination of channels and time steps.

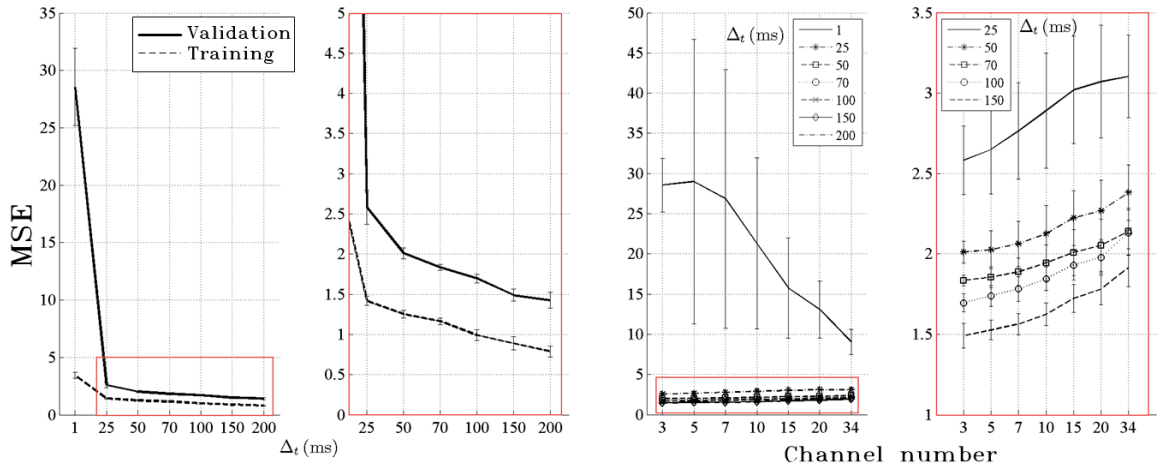

Figure 4. Error curve across volunteers respect to variations in parameters Δ_t (left) and number of channels C (right) for ascending tasks.

These graphics allow us to understand how parameters govern the decoding response. In summary, as the parameter Δ_t increases, the decoding precision augment as was shown in 4 left, on the other hand, increasing the number of channels in the data set makes that the decoding precision decays, increasing the *MSE* in an interval from 25 to 150 ms (red square), meanwhile, when $\Delta_t = 1$ the decoding precision improves with the augment of the channels, however is not sufficient to equate the response with the previous interval.

4.2 State estimation

According to the previous test, was selected as configuration parameters, the set of 3 channels and a Δ_t of 70 ms. The motion data set were extracted from the movement data of each volunteer, selecting for one, those trajectories whose resultant $|\mathbf{A}|$ of the state model were minor of 3, and the second with the remaining movements. This criterion was done as the trajectories with lower norm are resultant from data sets of lower variance Veslin *et al.* (2019). The compiled results in this section show the response of the validation set in Fig. 5. A decoding example is presented for an ascending (left), and a descending (right) tasks, in this figure, the bold line indicates the real value for position x_1, velocity x_2, and acceleration x_3, and the dashed line is the state estimation $\hat{\mathbf{x}}$. According to the *MSE* value, is observed that the descending movements had better decoding response that the ascending ones, meanwhile acceleration presents the lower decoding response for both tasks, followed by velocity and position.

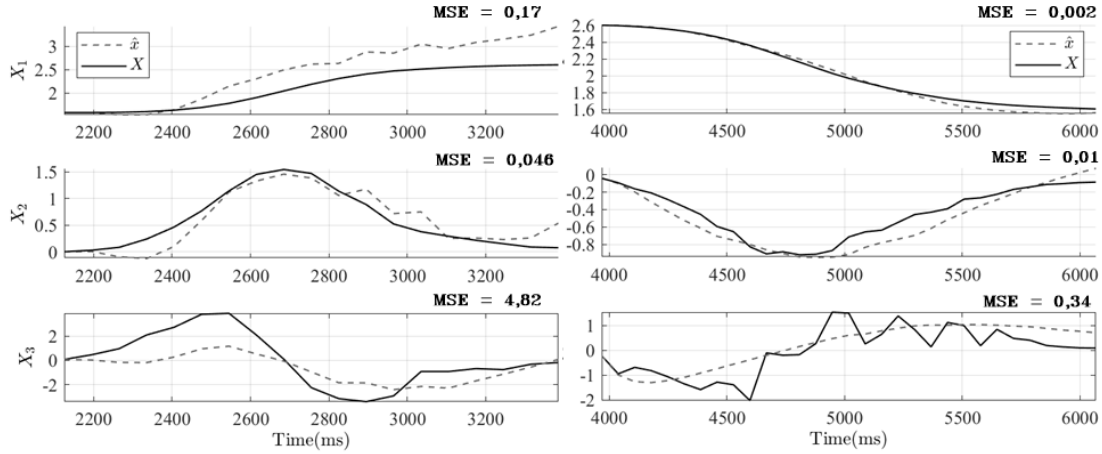

Figure 5. Decoding for ascending (left) and descending (right) imaginary movements.

In the box-plot of Fig. 6 right is presented the state's *MSE* distribution for all the volunteers when trajectories whit $|\mathbf{A}| < 3$ were used, it describes the distribution of the *MSE* resulting from the validation fold. The acceleration presented worse distribution with a mean *MSE* around 5 and a high variance up to 11. Meanwhile, velocity and position presented better decoding response whit mean closer to zero and lower variance in comparison with the acceleration. In the left, is presented a dispersion graphics associating the trained matrix $\mathbf{A}$ with the mean decoding error of the tree states, no significant variations were found respect to the magnitude of this value and the *MSE* value between the volunteers.

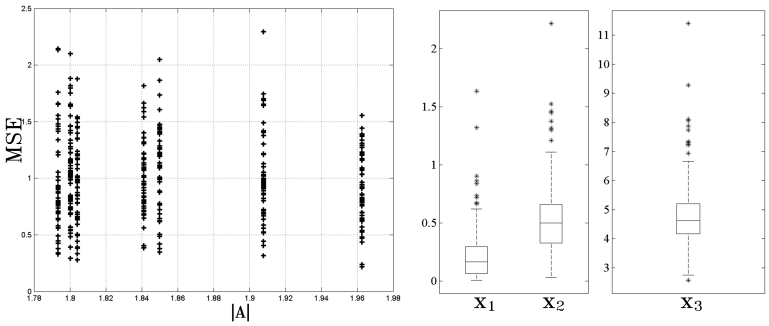

Figure 6. In the left, a dispersion graphic describe the mean *MSE* response for decoding imaginary ascendant task when $|\mathbf{A}| < 3$. In the right a box-plot describe the variation of each estate.

In Fig. 7 (left) is presented the variation of the resultant trained matrix $\mathbf{A}$ respect the mean decoding error of the tree states when trajectories with $|\mathbf{A}| > 3$ were chosen. An increment in the decoding error is presented around the three states, oscillating the *MSE* response between 2 an 9. This increment is observed in the detailed box-plot of Fig 7 (right). The *MSE* error distribution presented a higher dispersion, increasing the decoding error of the velocity and acceleration states. The position did not experience major variation respecting the observed in Fig. 6 but is visible that the box distribution passed the *MSE* one value for this figure.

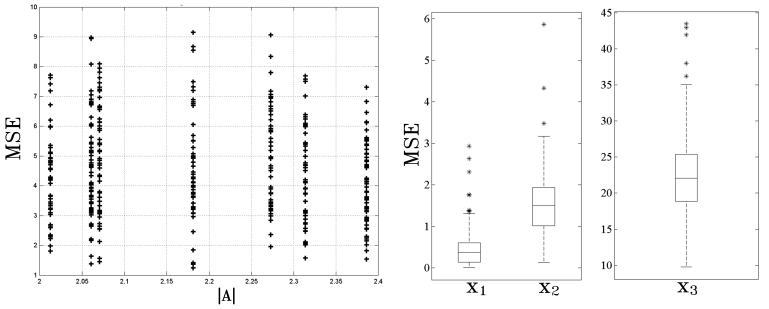

Figure 7. In the left, a dispersion graphic describe the mean *MSE* response for decoding imaginary ascendant task when $|\mathbf{A}| > 3$. In the right a box-plot describe the variation of each estate.

5. Discussion

In this work, the Kalman Filter was used to decode imaginary elbow motion from non-invasive *EEG*. To do that, an experimental protocol that commanded the execution of real and imaginary task was performed. A training data coming from the protocol was built, from real trials, the time interval and the performed movement were extracted, meanwhile from imaginary trials, the *EEG* signals related to the task were used.

In Fig. 4 was presented the error curves related to the parameter evaluation. Was found that exist an optimal interval of $25 \leq \Delta_t \geq 200ms$ around the 7 volunteers with lower *MSE*. Also, it was found that increasing the number of channels for that specific interval leads to a decreasing of the decoding accuracy. The results showed that only with *EEG* channels C_3, C_5 and C_1 it was possible to improve the best decoding response from imaginary motion. This result was the same obtained in Veslin *et al.* (2019), according to this, the addition of channels with lower coherence does not seems to expand the decoding properties, increasing the over-fitting over trials, in Fig. 8 is presented the coherence value over channels respect to C_3, it is observed that channels C_5 and C_1 presented a coherence value closer to $0,9$ descending over the channels in a linear form.

The selected three channels also, presented a lower variance in the decoding response among volunteers, as was shown in the vertical bars of Fig. 4-right. Therefore, this generalization provided the best response over trials and also over volunteers, Indicating first, that decoding results improve when related neural groups had common responses, and also, that the consideration of other brain areas depends on the voluntary responses, requiring of specific analysis to evaluate if their addition helps to improve the decoding capabilities of the filter.

The error curves of Fig. 4 also gave us an insight into the influence of parameter Δ_t for the state estimation. When its values increased, it led to a diminution in the decoding error for both ascending and descending movements. This result was similar to the found in Wu *et al.* (2002), were decoding response increased with an augment of the time step, indicating that movements described with fewer points are closer to the linear consideration done for the propagation model. However, decoding with high Δ_t values could affect the movement control when fast response *BMI* systems are required.

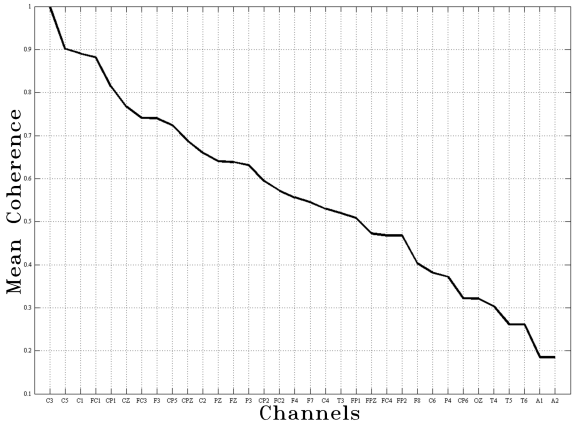

Figure 8. Mean coherence through trials from the c-channel respect to C_3.

The individual results after the parameter selection (Fig.5) showed that acceleration is the state with the worst decoding response having the highest mean *MSE* value and variance (Fig. 6). This response was also presented into the decoding of real motion Veslin *et al.* (2019) and using invasive *EEG* Wu *et al.* (2006), who found that this motion appears not to be encoded in neural firing rates. However, it was possible to reduce the decoding error with a proper trial selection. In Fig. 7 was presented a new decoding response using trials with $|\mathbf{A}| > 3$, the decoded error increased with respect to the previous test.

This propagation of the decoding error with respect to $|\mathbf{A}|$ is evidenced when Fig. 6 and Fig. 7 are compared. Both graphics presented the mean *MSE* variation in each volunteer. The line distribution was caused by the use of the same trajectory over trials. Hence, each volunteer trained their matrix $\mathbf{A}$ according to the mean movement obtained. When $|\mathbf{A}| < 3$ the decoding error was decreased not only into the acceleration but also in velocity and position, reducing the mean decoding error and their variance. In Fig. 7 the mean *MSE* error variance goes up to 8 in almost all volunteers, when in Fig. 6 is observed that *MSE* barely ultra-passes 2.

Previously Korik *et al.* (2018) proved that is possible to decode imaginary movement with non-invasive *EEG*, using linear filters to estimate 2-D hand movement with high accuracy (a correlation value of 0.972), also demonstrating that alpha y beta bands are capable of being used to decode imaginary (and real) movement. In this work, we use the alpha band to decode not only position but also velocity and acceleration, applying the Kalman Filter and using an alternative experimental paradigm to decode another movement. We also showed that the selection of a proper data set could improve the decoding precision of the filter, reducing the estimation error through the validation of the resulting $|\mathbf{A}|$ matrix. The filter precision also could be configured through the proper selection of the channels quantity and the time step of the signals used to train the filter models.

The generalization of both parameters and the use of a proper set of movements allowed to reduce the decoding error of imaginary motion in 7 volunteers, these results prove the fact that decoding motion with Kalman filter is strongly dependent of the data set configurations not only in real motion (Veslin *et al.* (2019)) but also in imaginary tasks. Therefore, it is necessary to build data set configurations with a lower variance to reduce decoding error.

The filter's linearity may cause a considerable difference between both data set. Thus, non-linear models as the Extended Kalman Filter, or even, neural networks could develop models that are not influenced by motion variability, and therefore, being able to decode a broad set of variations.

6. Conclusion

In this work, the Kalman filter was tested to decode imaginary elbow movement using non-invasive *EEG* signals using experimental data from real movements. The experimental result showed us that it is possible to decode this movement with relative precision. An optimal configuration for the state and measurement signals was made through a set of parameters (number of channels and time step), allowing us to find the best estimation through cross-validation.

A set of analysis was made using the optimal set of parameters and was found that the capability to estimate different movements by the filter appears to be affected by the trained state model. Decoding results from the resultant $\mathbf{A}$ matrix coefficient with minor norm presented lower decoding results than those who used a trained matrix with a higher norm.

The presented results gave an insight into how Kalman filter works and how the training set could be configured through a rigorous selection of trials to improve decoding results. Therefore, the information could be removed according to the response of the volunteer, if it does not cope with the task regularity. However, future works must be aimed to improve the decoding results using highly variable data, and therefore, augmenting the capabilities of the filter to detect different intents of motion.

7. ACKNOWLEDGMENTS

The authors would like to thank FINEP, CNPq, FAPERJ, Fundação COPPETEC, and DIPPG/CEFET-RJ for supporting our work. As well the students Edwiges Beatriz Coimbra de Souza, Aline Macedo Rocha Rodriguez, and Andre Silva for their helping in the *EEG* data acquisition, and Marco Vinicio Chiorri for their technical assistance.

8. REFERENCES

Alazrai, R., Alwanni, H. and Daoud, M.I., 2019. "Eeg-based bci system for decoding finger movements within the same hand". *Neuroscience letters*, Vol. 698, pp. 113–120.

Besserve, M., Jerbi, K., Laurent, F., Baillet, S., Martinerie, J. and Garnero, L., 2007. "Classification methods for ongoing eeg and meg signals". *Biological research*, Vol. 40, No. 4, pp. 415–437.

Cassim, F., Szurhaj, W., Sediri, H., Devos, D., Bourriez, J.L., Poirot, I., Derambure, P., Defebvre, L. and Guieu, J.D., 2000. "Brief and sustained movements: differences in event-related (de) synchronization (erd/ers) patterns". *Clinical neurophysiology*, Vol. 111, No. 11, pp. 2032–2039.

Frolov, A., Húsek, D., Bobrov, P., Mokienko, O. and Tintera, J., 2013. "Sources of electrical brain activity most relevant to performance of brain-computer interface based on motor imagery". *Brain-Computer Interface Systems-Recent Progress and Future Prospects*, pp. 175–193.

Georgopoulos, A.P., Schwartz, A.B. and Kettner, R.E., 1986. "Neuronal population coding of movement direction". *Science*, Vol. 233, No. 4771, pp. 1416–1419.

Hochberg, L.R., Bacher, D., Jarosiewicz, B., Masse, N.Y., Simeral, J.D., Vogel, J., Haddadin, S., Liu, J., Cash, S.S., van der Smagt, P. *et al.*, 2012. "Reach and grasp by people with tetraplegia using a neurally controlled robotic arm". *Nature*, Vol. 485, No. 7398, p. 372.

Homer, M.L., Harrison, M.T., Black, M.J., Perge, J.A., Cash, S.S., Friehs, G. and Hochberg, L.R., 2013. "Mixing decoded cursor velocity and position from an offline kalman filter improves cursor control in people with tetraplegia". In *Neural Engineering (NER), 2013 6th International IEEE/EMBS Conference on*. IEEE, pp. 715–718.

Jeon, Y., Namb, C.S., Kim, Y.J. and Whang, M.C., 2011. "Event-related (de)synchronization (erd/ers) during motor imagery tasks: Implications for brainecomputer interfaces". *Int. J. Ind. Ergon.*, Vol. 41, pp. 428–436.

Kim, J.H., Bießmann, F. and Lee, S.W., 2014. "Decoding three-dimensional trajectory of executed and imagined arm movements from electroencephalogram signals". *IEEE Transactions on Neural Systems and Rehabilitation Engineering*, Vol. 23, No. 5, pp. 867–876.

Korik, A., Siddique, N., Sosnik, R. and Coyle, D., 2014. "Correlation of eeg band power and hand motion trajectory". In *Proceedings of the 6th international brain-computer interface conference*.

Korik, A., Sosnik, R., Siddique, N. and Coyle, D., 2018. "Decoding imagined 3d hand movement trajectories from eeg: Evidence to support the use of mu, beta, and low gamma oscillations". *Frontiers in Neuroscience*, Vol. 12, p. 130. ISSN 1662-453X. doi:10.3389/fnins.2018.00130. URL `https://www.frontiersin.org/article/10.3389/fnins.2018.00130`.

Lalitharatne, T.D., Teramoto, K., Hayashi, Y. and Kiguchi, K., 2013. "Towards hybrid eeg-emg-based control approaches to be used in bio-robotics applications: Current status, challenges and future directions". *Paladyn, Journal of Behavioral Robotics*, Vol. 4, No. 2, pp. 147–154.

Lalitharatne, T.D., Yoshino, A., Hayashi, Y., Teramoto, K. and Kiguchi, K., 2012. "Toward eeg control of upper limb power-assist exoskeletons: A preliminary study of decoding elbow joint velocities using eeg signals". In *Micro-NanoMechatronics and Human Science (MHS), 2012 International Symposium on*. IEEE, pp. 421–424.

Lana, E.P., Adorno, B.V. and Tierra-Criollo, C.J., 2015. "Detection of movement intention using eeg in a human-robot interaction environment". *Research on Biomedical Engineering*, Vol. 31, No. 4, pp. 285–294.

Li, M.A., Wang, Y.F., Jia, S.M., Sun, Y.J. and Yang, J.F., 2019. "Decoding of motor imagery eeg based on brain source estimation". *Neurocomputing*, Vol. 339, pp. 182–193.

Luu, T.P., He, Y., Brown, S., Nakagome, S. and Contreras-Vidal, J.L., 2016. "Gait adaptation to visual kinematic perturbations using a real-time closed-loop brain–computer interface to a virtual reality avatar". *Journal of neural engineering*, Vol. 13, No. 3, p. 036006.

Lv, J., Li, Y. and Gu, Z., 2010. "Decoding hand movement velocity from electroencephalogram signals during a drawing task". *Biomedical engineering online*, Vol. 9, No. 1, p. 1.

Moorman, H.G., Gowda, S. and Carmena, J.M., 2017. "Control of redundant kinematic degrees of freedom in a closed-loop brain-machine interface". *IEEE Transactions on Neural Systems and Rehabilitation Engineering*, Vol. 25, No. 6, pp. 750–760.

Moran, D.W. and Schwartz, A.B., 1999. "Motor cortical activity during drawing movements: population representation during spiral tracing". *Journal of neurophysiology*, Vol. 82, No. 5, pp. 2693–2704.

Müller-Putz, G., Schwarz, A., Pereira, J. and Ofner, P., 2016. "From classic motor imagery to complex movement intention decoding: The noninvasive graz-bci approach". In *Progress in brain research*, Elsevier, Vol. 228, pp. 39–70.

Noback, C.R., Strominger, N.L., Demarest, R.J. and Ruggiero, D.A., 2005. *The Human Nervous System: Structure and Function*. Humana Press Inc, sixth edition edition.

Ofner, P. and Müller-Putz, G.R., 2012. "Decoding of velocities and positions of 3d arm movement from eeg". In *2012 Annual International Conference of the IEEE Engineering in Medicine and Biology Society*. IEEE, pp. 6406–6409.

Ofner, P. and Müller-Putz, G.R., 2015. "Using a noninvasive decoding method to classify rhythmic movement imaginations of the arm in two planes". *IEEE transactions on biomedical engineering*, Vol. 62, No. 3, pp. 972–981.

Pfurtscheller, G., Brunner, C., Schlo, A. and da Silva, F.L., 2006. "Mu rhythm (de)synchronization and eeg single-trial classification of different motor imagery tasks". *NeuroImage*, Vol. 31, p. 153 – 159.

Pfurtscheller, G. and da Silva, F.L., 1999. "Event-related eeg/meg synchronization and desynchronization: basic principles". *Clin. Neurophysiol.*, Vol. 110, pp. 1842 – 1857.

Pistohl, T., Ball, T., Schulze-Bonhage, A., Aertsen, A. and Mehring, C., 2008. "Prediction of arm movement trajectories from ecog-recordings in humans". *Journal of neuroscience methods*, Vol. 167, No. 1, pp. 105–114.

Ramos-Murguialday, A. and Birbaumer, N., 2015. "Brain oscillatory signatures of motor tasks". *Journal of neurophysiology*, Vol. 113, No. 10, pp. 3663–3682.

Rao, R.P., 2019. "Towards neural co-processors for the brain: combining decoding and encoding in brain–computer interfaces". *Current opinion in neurobiology*, Vol. 55, pp. 142–151.

Robinson, N., Guan, C. and Vinod, A., 2015. "Adaptive estimation of hand movement trajectory in an eeg based brain–computer interface system". *Journal of neural engineering*, Vol. 12, No. 6, p. 066019.

Robinson, N., Vinod, A.P., Ang, K.K., Tee, K.P. and Guan, C.T., 2013. "Eeg-based classification of fast and slow hand movements using wavelet-csp algorithm". *IEEE Transactions on Biomedical Engineering*, Vol. 60, No. 8, pp. 2123–2132.

Robinson, N. and Vinod, A., 2016. "Noninvasive brain-computer interface: Decoding arm movement kinematics and motor control". *IEEE Systems, Man, and Cybernetics Magazine*, Vol. 2, No. 4, pp. 4–16.

Roy, R., Mahadevappa, M. and Kumar, C., 2016. "Trajectory path planning of eeg controlled robotic arm using ga". *Procedia Computer Science*, Vol. 84, pp. 147–151.

Salvaris, M. and Sepulveda, F., 2010. "Classification effects of real and imaginary movement selective attention tasks on a p300-based brain–computer interface". *Journal of neural engineering*, Vol. 7, No. 5, p. 056004.

Shakibaee, F., Mottaghi, E., Kobravi, H.R. and Ghoshuni, M., 2019. "Decoding knee angle trajectory from electroencephalogram signal using narx neural network and a new channel selection algorithm". *Biomedical Physics & Engineering Express*.

Soekadar, S.R., Witkowski, M., Vitiello, N. and Birbaumer, N., 2015. "An eeg/eog-based hybrid brain-neural computer interaction (bnci) system to control an exoskeleton for the paralyzed hand". *Biomedical Engineering/Biomedizinische Technik*, Vol. 60, No. 3, pp. 199–205.

Tang, Z., Zhang, K., Sun, S., Gao, Z., Zhang, L. and Yang, Z., 2014. "An upper-limb power-assist exoskeleton using proportional myoelectric control". *Sensors*, Vol. 14, No. 4, pp. 6677–6694.

Tayeb, Z., Fedjaev, J., Ghaboosi, N., Richter, C., Everding, L., Qu, X., Wu, Y., Cheng, G. and Conradt, J., 2019. "Validating deep neural networks for online decoding of motor imagery movements from eeg signals". *Sensors*, Vol. 19, No. 1, p. 210.

Ubeda, A., Costa, A., Iánez, E., Piñuela-Martín, E., Márquez-Sánchez, E., del Ama, A.J., Gil-Agudo, Á. and Azorín, J.M., 2015. "Single joint movement decoding from eeg in healthy and incomplete spinal cord injured subjects". In *Intelligent Robots and Systems (IROS), 2015 IEEE/RSJ International Conference on*. IEEE, pp. 6179–6183.

Veslin, E., Dutra, M., Bevilacqua, L., Raptopoulos, L., Andrade, WS and Soares, J., 2019. "Decoding elbow movement with kalman filter using non-invasive eeg". In *2019 IEEE 2nd Colombian Conference on Applications in Computational Intelligence (ColCACI)*. pp. 1–6.

Wu, W., Black, M., Gao, Y., Bienenstock, E., Serruya, M. and Donoghue, J., 2002. "Inferring hand motion from multi-cell recordings in motor cortex using a kalman filter". In *SAB'02-workshop on motor control in humans and robots: On the interplay of real brains and artificial devices*. pp. 66–73.

Wu, W., Gao, Y., Bienenstock, E., Donoghue, J.P. and Black, M.J., 2006. "Bayesian population decoding of motor cortical activity using a kalman filter". *Neural computation*, Vol. 18, No. 1, pp. 80–118.

Xu, L. and Adler, A., 2004. "An improved method for muscle activation detection during gait". In *Electrical and Computer Engineering, 2004. Canadian Conference on*. IEEE, Vol. 1, pp. 357–360.

Zhang, R., Li, Y., Yan, Y., Zhang, H., Wu, S., Yu, T. and Gu, Z., 2016. "Control of a wheelchair in an indoor environment based on a brain–computer interface and automated navigation". *IEEE transactions on neural systems and rehabilitation engineering*, Vol. 24, No. 1, pp. 128–139.

9. RESPONSIBILITY NOTICE

The authors are the only responsible for the printed material included in this paper.